

Progression of Cerebral White Matter Hyperintensities and the Associated Sonographic Index¹

Woo-Jin Lee, MD
Keun-Hwa Jung, MD, PhD
Young Jin Ryu, MD
Keon-Joo Lee, MD
Jeong-Min Kim, MD, PhD
Soon-Tae Lee, MD, PhD
Kon Chu, MD, PhD
Manho Kim, MD, PhD
Sang Kun Lee, MD, PhD
Jae-Kyu Roh, MD, PhD

Purpose:

To evaluate the relationship between penetrating arterial pulsation and the progression of white matter hyperintensities (WMHs) by using the sonographic resistance index (RI) along the M1 segment of the middle cerebral artery (MCA).

Materials and Methods:

The study design was approved by the institutional review board of Seoul National University Hospital. The study included 450 individuals who had undergone initial transcranial Doppler (TCD) sonography and magnetic resonance imaging, with follow-up imaging performed within 34–45 months, and who had no stenosis of 30% or more in the internal carotid artery or MCA or a history of stroke other than an old lacunar infarction. MRIR was defined as distal RI divided by proximal RI, where the distance between proximal M1 and distal M1 was approximately 20 mm based on TCD evaluation. WMH progression was quantitatively evaluated by subtracting WMH volume at baseline from WMH volume at follow-up.

Results:

At baseline, mean MRIR was 0.974 ± 0.045 (standard deviation), and mean WMH volume was $9.66 \text{ mL} \pm 14.54$. After a mean of $38.3 \text{ months} \pm 3.4$, the WMH volume change was $4.06 \text{ mL} \pm 7.35$. WMH volume change was linearly associated with MRIR ($r = 0.328$, $P < .001$), along with the baseline WMH volume ($r = 0.433$, $P < .001$) and mean MCA pulsatility index ($r = 0.275$, $P = .037$). MRIR values greater than or equal to 1.000 were associated with a greater increase in WMH volume ($P < .001$).

Conclusion:

MRIR might reflect the pulsation of penetrating arteries and is independently associated with WMH progression.

©RSNA, 2017

Online supplemental material is available for this article.

¹From the Departments of Neurology (W.J.L., K.H.J., K.J.L., S.T.L., K.C., M.K., S.K.L., J.K.R.) and Radiology (Y.J.R.), Seoul National University Hospital, 101 Daehangno, Jongno-gu, Seoul 110-744, South Korea; Program in Neuroscience, Neuroscience Research Institute of SNUMRC, College of Medicine, Seoul National University, Seoul, South Korea (K.H.J., S.T.L., K.C., M.K., S.K.L.); Department of Neurology, Chung-Ang University Hospital, Seoul, South Korea (J.M.K.); and Department of Neurology, the Armed Forces Capital Hospital, Sungnam, South Korea (J.K.R.). Received September 3, 2016; revision requested November 4; revision received November 30; accepted January 11, 2017; final version accepted January 31. **Address correspondence to K.H.J.** (e-mail: jungkh@gmail.com).

Supported by Seoul National University Hospital (04-2015-0880) and Ministry of Science, ICT and Future Planning (2016M3C7A1914002).

©RSNA, 2017

Cerebral white matter hyperintensities (WMHs) are prevalent in elderly individuals and have substantial clinical implications (1). Increased age and hypertension have been shown to be related to WMH severity, but they do not account for much of the risk (1–4). The relevance of other conventional cerebrovascular risk factors to WMH is also uncertain (1,3–6) since the mechanism of WMH progression is distinct from that of large artery atherosclerosis (1,7,8). Although not fully elucidated, increasing evidence indicates that WMH progression is a consequence of impaired solute clearance via the perivascular glymphatic system around the cortical penetrating arteries (1,7–10). Furthermore, because the solute clearance is mainly driven by pulsation of the penetrating arteries, age-related reduction of compliance in those vessels (luminal distensibility per a given intraluminal pressure increment) (11) is increasingly recognized as

the fundamental mechanism underlying WMH progression (7–10,12).

Because the pulsatility of the penetrating arteries has different physiologic properties from those of large pial arteries (8), it is necessary to identify a measurable index of penetrating arterial compliance to facilitate proper prognostication and to alleviate WMH progression. However, to our knowledge, the role of penetrating arterial compliance in WMH progression has not been elucidated in patients. Biomarkers of systemic vascular stiffness have been investigated in relation to WMH progression (13,14); however, those markers represent only systemic large artery compliance. The pulsatility index (PI) at the M1 portion of the middle cerebral arteries (MCAs) also has been suggested to be a cerebrovascular compliance marker (15). However, in consideration of the fact that M1 is a large artery (approximately 2.8–3.0 mm in diameter) with low resistance and that its diameter remains nearly constant in response to changes in intravascular pressure (16), an increased PI would reflect the systemic pulse pressure accentuation delivered to M1 rather than the reduced compliance of the cerebral penetrating arteries.

A previous study suggested that the ratio of the resistance index (RI) decrement to decreases in distal arterial resistance represents the actual vascular compliance (11); however, there are limitations to its clinical interpretation. Additionally, a recent study showed that PI in large cerebral arteries decreases as it moves from proximal to distal, and the

reduction of dampening capacity is associated with increasing age and increased microvascular damage (17). Since the diameter change in M1 is negligible (16) and since the relationship between flow volume and blood velocity in M1 is nearly linear (18), RI approximately represents the ratio of additional flow delivered by a systolic pulse.

The penetrating arteries from M1 are the main blood supplier to the periventricular white matter, and they are a major supplier to the subcortical white matter (19); therefore, their flow variation during a pulse cycle, which could be evaluated by calculating the RI ratio along M1 (MRIR), might be an indicator of WMH progression. Hence, this study aimed to evaluate the relationship between penetrating arterial pulsation and the progression of WMH by using the sonographic index MRIR.

Advances in Knowledge

- A sonographic marker of cerebral microvascular compliance, resistance index ratio along the middle cerebral artery (MCA) (MRIR), can be used to evaluate the compliance of perforating arterioles from the M1 segment of the MCA.
- MRIR was linearly associated with cerebral white matter hyperintensity (WMH) progression ($P < .001$) along with the baseline WMH volume ($P < .001$) and mean MCA pulsatility index (MMPI) ($P = .037$) after adjustment for factors known to affect cerebral WMH progression (ie, increasing age and conventional cerebrovascular risk factors).
- Linear association between the MRIR and WMH volume progression was significant for both periventricular and deep WMH ($P < .001$ for periventricular WMH, $P = .004$ for deep WMH); however, the association was higher for periventricular WMH progression.

Implications for Patient Care

- MRIR can be used as a marker of cerebral microvascular compliance and to predict or monitor the long-term progression of cerebral WMH.
- A cutoff MRIR might be used as an indicator of diminished cerebral microvascular compliance, as an MRIR greater than or equal to 1.000 was strongly associated with significant WMH progression in this study.

Materials and Methods

Study Population and Follow-up

This study was reviewed and approved by the institutional review board of

<https://doi.org/10.1148/radiol.2017162064>

Content code: **NR**

Radiology 2017; 284:824–833

Abbreviations:

ACEi = angiotensin-converting enzyme inhibitor
ARB = aldosterone receptor blocker
MCA = middle cerebral artery
MMPI = mean MCA pulsatility index
MRIR = RI ratio along the MCA
PI = pulsatility index
RI = resistance index
TCD = transcranial Doppler
WMH = white matter hyperintensity

Author contributions:

Guarantors of integrity of entire study, W.J.L., K.H.J.; study concepts/study design or data acquisition or data analysis/interpretation, all authors; manuscript drafting or manuscript revision for important intellectual content, all authors; approval of final version of submitted manuscript, all authors; agrees to ensure any questions related to the work are appropriately resolved, all authors; literature research, K.H.J., Y.J.R., K.J.L., K.C., M.K., S.K.L., J.K.R.; clinical studies, W.J.L., K.J.L., J.M.K., S.T.L., J.K.R.; statistical analysis, Y.J.R., J.M.K.; and manuscript editing, W.J.L., K.H.J., K.C., M.K., S.K.L.

Conflicts of interest are listed at the end of this article.

Seoul National University Hospital. Informed consent was waived, as patient medical information was made anonymous and deidentified by an author (K.H.J.) directly after it was obtained by permanently deleting the patient number and substituting it with a random subject number generated by using Excel software (Microsoft, Redmond, Wash).

We retrospectively evaluated individuals who visited a tertiary hospital and underwent brain magnetic resonance (MR) imaging, MR angiography, and transcranial Doppler (TCD) sonography within a 3-month interval and who underwent follow-up MR imaging or MR angiography within 34–45 months after the initial evaluation between January 2005 and March 2012. Our search initially identified 1033 individuals. To minimize a potential source of bias that might have influenced WMH progression, patients were excluded if they (*a*) were younger than 50 years; (*b*) were incapable of independent daily living; (*c*) had a stenosis of 30% or more in the intra- or extracranial internal carotid arteries or MCAs at initial MR angiography; (*d*) had prior history or interval development of a chronic systemic illness; (*e*) had a stroke with a cause other than lacunar infarction, intra-arterial intervention, intracranial or neck radiation therapy, major head trauma, or a recent (≤ 90 days) lacunar stroke; (*f*) had central nervous system inflammatory or degenerative disorders; and (*g*) had a poor temporal window for TCD or poor MR image quality. Patients with a history of lacunar infarction were included to cover various baseline WMH severities in the study population. On the basis of these criteria, 450 patients qualified for the final analysis (Table E1 [online]). The indications for the baseline MR imaging and TCD evaluations were part of a regular medical check-up program provided by the Seoul National University Hospital Healthcare System in 186 (41.3%) patients, evaluation for headache or dizziness in 118 (26.2%), follow-up of one small (≤ 3 mm) unruptured intracranial aneurysm in 33 (7.3%), and follow-up of an old lacunar infarction in 113 (25.1%). Indications for follow-up MR imaging or MR angiography included a

regular medical check-up program in 186 (41.3%) patients, follow-up of baseline WMH in 82 (18.2%), follow-up of one small unruptured aneurysm in 40 (8.9%), and follow-up of an old lacunar infarction in 142 (31.6%) (Table E2 [online]).

Patient medical records were evaluated to obtain clinical information, including age; sex; presence of hypertension, diabetes mellitus, hyperlipidemia, or coronary heart disease; previous stroke history; smoking in the previous 5 years; and use of statins (1), an angiotensin-converting enzyme inhibitor (ACEi) or aldosterone receptor blocker (ARB) (20), or antiplatelet agents during the follow-up period (1).

Transcranial Doppler Analysis

Intracranial arteries were sonographically evaluated by using a 2-MHz pulsed-wave and range-gated TCD probe (Digital PMD 100 or ST3 Digital PMD 150; Spencer Technologies, Redmond, Wash) with a 9-mm sample volume and a transmit power level of 100 mW/cm². The protocol was standardized for every patient and was conducted by two skilled sonographers with 10 and 8 years of experience. TCD data—including peak systolic velocity (PSV), minimal diastolic velocity (MDV), and mean flow velocity (MFV) (all were measured in centimeters per second); PI; and RI—were obtained along the M1 portion of the MCA (from the temporal windows with an insonation depth of 60–70 mm by identifying an approaching flow from the internal carotid artery bifurcation) with 5-mm distance of insonation depth for each obtained data set (21,22). The mean of 15 consecutive pulses was taken as the velocity value. We designated MRIR as the mean ratio of RI along M1 (distal RI to proximal RI) in each hemisphere, where the distance between proximal M1 and distal M1 was fixed as approximately 20 mm. The mean PI in both MCAs (MMPI) was defined as the mean of PIs at proximal and distal M1 (Fig 1).

MR Imaging

MR imaging was performed by using a 1.5-T MR imager with an eight-channel head coil (Philips Ingenia; Philips, Best, the Netherlands) or a 3.0-T MR

imager with a 16-channel head coil (Verio; Siemens, Erlangen, Germany). In every instance, the MR imaging protocol included T1- and T2-weighted, fluid-attenuated inversion recovery, and gradient-echo sequences; intracranial time-of-flight angiography, and either time-of-flight angiography of the neck or contrast material-enhanced MR angiography. Fluid-attenuated inversion recovery MR imaging was performed with the following parameters: repetition time msec/echo time msec, 9000–9900/97–163; section thickness, 4.0 mm; no section gap; 24–27 sections covering the entire brain; field of view, 240 mm \times 240 mm; and matrix, 220 \times 220. Common MR angiography parameters included a flip angle of 20° and a matrix of 384 \times 292. Time-of-flight MR angiography (20–25/3–7; field of view, 160 mm \times 160 mm) and contrast-enhanced MR angiography (7.3/2.5; field of view, 240 mm \times 240 mm) also were performed. In every patient, MR imaging protocols were identical at baseline and follow-up. Images were reviewed by a radiologist (Y.J.R., 6 years of experience) who was blinded to the clinical data, as follows: fluid-attenuated inversion recovery and MR angiography sequences were reviewed to evaluate the presence of or the mechanism underlying preexisting ischemic lesions. Gradient-echo sequences were used to identify preexisting intracerebral hemorrhage, and the three-dimensional reconstructed images acquired with time-of-flight or contrast-enhanced MR angiography were used to exclude subjects with stenosis of the MCA or internal carotid artery (23–25). Stenosis degree of more than 30% was used as a cutoff (23,24,26). It was measured at the angle in which the highest degree of stenosis was identified per the established methods for intra- and extracranial stenosis, which have been shown to be highly reproducible (23–25).

Volumetric Analysis

For volumetric analysis of the WMH burden, fluid-attenuated inversion recovery images were registered at an offline workstation. WMH was defined as hyperintense lesions without central hypointensity in the cerebral white matter,

Figure 1

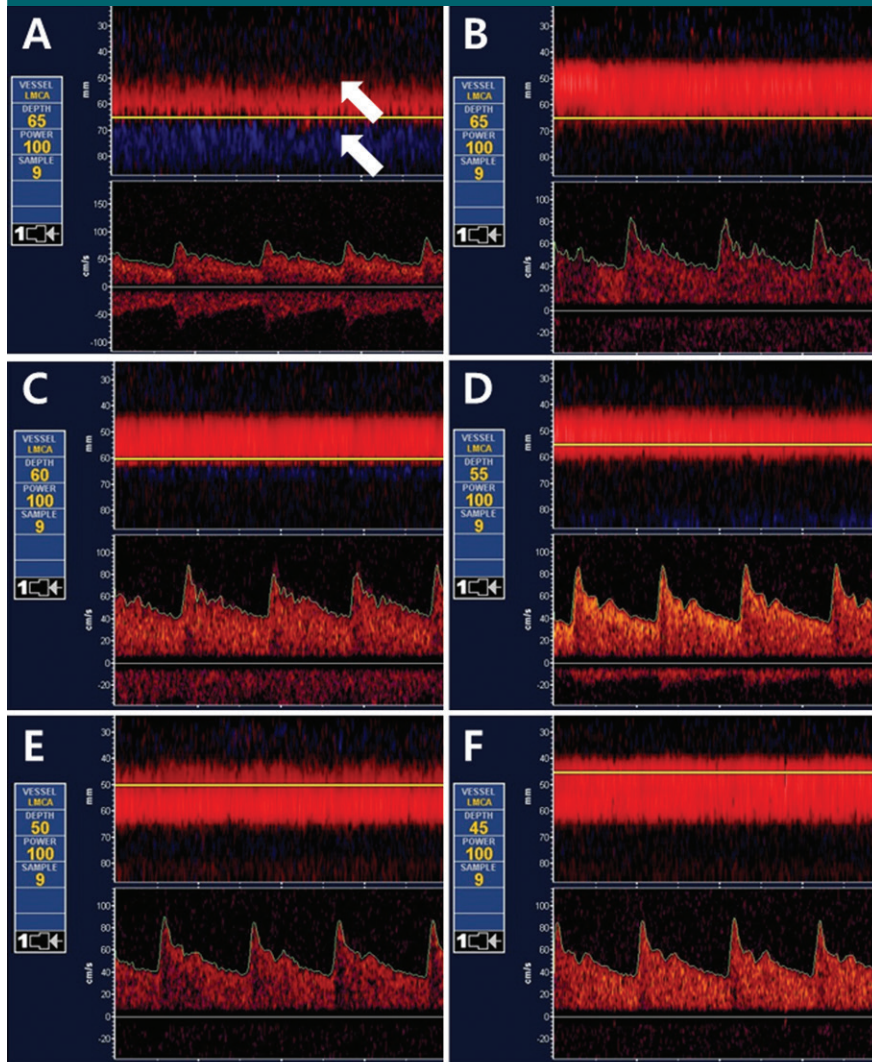


Figure 1: Schematic description of how sonographic parameters are obtained. A, Initially, MCA was identified as flow toward the probe at an insonation depth of 50–55 mm from the temporal windows. By slowly increasing insonation depth to 65–75 mm, bifurcation of the terminal internal carotid artery is identified as two flows, one going away from the probe and one going toward it (anterior cerebral artery and MCA, respectively) (arrows). B–F, By adjusting depth of insonation from this point, the entire length of M1 flow is followed (usually 30–35 mm to 65–75 mm) until the signal is divided into two or three branches (M2 of MCA) (21,22). Peak systolic velocity (PSV), minimum diastolic flow velocity (MDV), and mean flow velocity (MFV), all of which are measured in centimeters per second, were obtained from proximal to distal M1 with 5-mm intervals of insonation depth, as a routine evaluation procedure (21). RI and PI at each point were calculated as $RI = \frac{PSV - MDV}{MFV}$ and $PI = \frac{PSV - MDV}{MFV}$ (11,15). MRIR was defined as the mean value of the ratios of distal RI (insonation depth, 40–50 mm) to proximal RI (insonation depth, 60–70 mm) along the M1 of each hemisphere, where the distance between the two points was fixed as 20 mm. MMPI was evaluated by calculating the mean values of PI at four points (distal M1 and proximal M1 in each hemisphere).

were calculated by using NeuRoi software (30). The change in WMH volume was calculated by subtracting lesion volume on baseline MR images from lesion volume on follow-up MR images; all volumes were measured in random order.

Statistical Analyses

Statistical software (SPSS, version 21.0; SPSS, Chicago, Ill) was used for all statistical analyses. Data are reported as number and percentage of patients with a given finding, mean ± standard deviation, or the median and interquartile range, as appropriate. Correlations between continuous variables and WMH volume change were assessed by using Pearson correlation coefficients. For categorical variables, WMH volume changes were compared between two subgroups by using Student *t* tests or the Mann–Whitney *U* test. Variables with *P* < .15 in those univariate analyses were entered into a linear regression analysis. For linear regression analysis, baseline WMH volume was log transformed to obtain a normal distribution. The variance

$$MRIR = \frac{\left(\frac{RI_{Distal}}{RI_{Proximal}}\right)_{Right} + \left(\frac{RI_{Distal}}{RI_{Proximal}}\right)_{Left}}{2}$$

$$MMPI = \frac{(PI_{Proximal} + PI_{Distal})_{Right} + (PI_{Proximal} + PI_{Distal})_{Left}}{4}$$

which differentiates these WMHs from perivascular spaces or lacunar infarcts (1,27). Lesions were classified as periventricular WMHs if they were directly connected to the lateral ventricles and as deep WMHs if they were not (28,29); all lesions were outlined by a neurologist (W.J.L., 6 years of experience) using semiautomated freeware (NeuRoi;

Christopher Tench, Nottingham University, Nottingham, England) (30). Measurement was performed with the reader blinded to whether an image was a baseline or follow-up image and to other clinical information. Lesions located in the brain stem or cerebellum were excluded. The total volume of WMH lesions and total brain volume

inflation factor was used to assess a multicollinearity between variables. For all analyses, $P < .05$ was considered to indicate a significant difference.

Results

Among the 450 individuals included in this study (overall mean age, 65.9 years \pm 8.2; age range, 50–87 years), 226 (50.2%) were male (mean age, 66.2 years \pm 8.3) and 224 (49.8%) were female (mean age, 65.6 years \pm 8.2 years) ($P = .447$). Mean baseline WMH volume was 9.66 mL \pm 14.54 (mean, 6.52 mL \pm 9.65 in the periventricular region and 3.11 mL \pm 4.89 in the deep white matter region). Follow-up MR imaging was performed a mean of 38.3 months \pm 3.4 (range, 34–45 months) after initial MR imaging. At follow-up, the mean WMH volume change was 4.06 mL \pm 7.35 (mean, 3.15 mL \pm 5.74 in the periventricular region and 0.91 \pm 1.68 mL in the deep white matter region) (Table 1). Reproducibility for WMH volume change measurements was evaluated by reanalyzing 20 randomly allocated pairs of baseline and follow-up MR images and was

Table 1

Demographic, Clinical, Sonographic, and Radiologic Profiles of the Study Population

Characteristic	Finding
Age (y)*	65.9 \pm 8.2
Male sex†	226 (50.2)
Previous stroke†	117 (26.0)
Hypertension†	287 (63.8)
Diabetes mellitus†	140 (31.1)
Coronary heart disease†	49 (10.9)
Smoking in past 5 years†	48 (10.7)
Hyperlipidemia†	154 (34.2)
Use of statins†	242 (53.8)
ACEi or ARB use†	202 (44.9)
Use of antiplatelet agents†	340 (75.6)
MMPI*	0.942 \pm 0.168
MRIR*	0.974 \pm 0.045
Baseline total WMH volume (mL)‡	9.66 \pm 14.54 (3.72) [1.25–13.87]
Periventricular WMH volume (mL)‡	6.52 \pm 9.65 (2.89) [0.97–9.21]
Deep WMH volume (mL)‡	3.11 \pm 4.89 (0.84) [0.28–4.60]
MR imaging interval (mo)*	38.3 \pm 3.4
WMH total volume change (mL)‡	4.06 \pm 7.35 (1.17) [0.09–4.93]
Periventricular WMH volume change (mL)‡	3.15 \pm 5.74 (0.85) [0.07–3.85]
Deep WMH volume change (mL)‡	0.91 \pm 1.68 (0.30) [0.03–1.10]
Lacunar infarction†	20 (4.4)

* Data are mean \pm standard deviation.

† Data are number of patients, with parentheses in percentages.

‡ Data are mean \pm standard deviation, with median in parentheses and interquartile range in brackets.

Figure 2

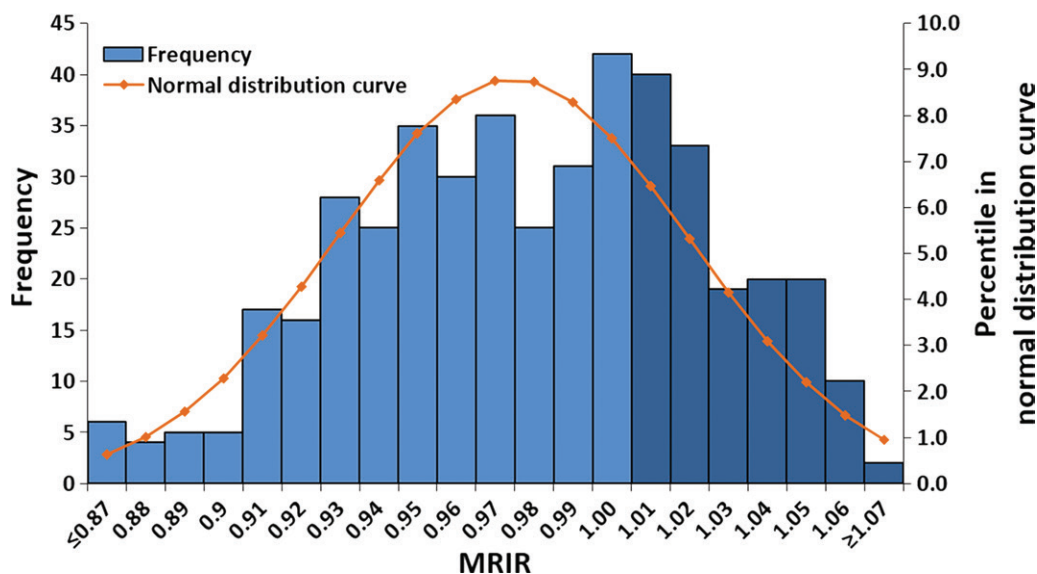


Figure 2: Distribution of study population according to MRIR values. Bar graph denotes the number of patients in each subgroup defined by intervals of MRIR value. A total of 144 (32.0%) patients had an MRIR greater than 1.00 (dark blue bars). Normal distribution curve is also shown

0.999 (95% confidence interval: 0.998, 1.000) for both deep and periventricular WMH volume changes. In TCD analyses, mean MMPI was 0.942 ± 0.168 (range, 0.575–1.437), and mean MRIR was 0.974 ± 0.045 (range, 0.846–1.136). A total of 144 (32.0%) of 450 patients had MRIR values of 1.000 or greater (Fig 2). The intraclass correlation coefficient of MRIR, evaluated with the 20 pairs of short-term (obtained within 12 weeks of interval) repetitive TCD studies from the study population, was strong (mean, 0.882; 95% confidence interval: 0.732, 0.948).

Correlation analyses revealed that WMH volume change was associated with age, baseline WMH volume, MRIR, and MMPI ($P < .001$ for all) (Table 2). In the univariate analyses for categorical parameters, hypertension ($P < .001$), diabetes mellitus ($P = .008$), hyperlipidemia ($P = .045$), prior use of ACEi or ARB ($P = .006$), prior use of antiplatelet agents ($P = .014$), and indications for initial MR imaging or TCD evaluations, only follow-up of an old lacunar infarction ($P = .002$) was associated with a higher WMH volume change (Table 3).

In the subsequent multivariate linear regression analysis adjusting for the total brain volume and the follow-up MR imaging intervals, total WMH volume change was linearly associated with MRIR ($P < .001$), along with the log value of baseline WMH volume ($P < .001$) and MMPI ($P = .037$). However, age ($P = .078$), history of lacunar infarction ($P = .294$), hypertension ($P = .468$), diabetes mellitus ($P = .236$), hyperlipidemia ($P = .311$), use of ACEi or ARB ($P = .951$), and use of antiplatelet agents ($P = .583$) were no longer significantly associated with WMH progression. When linear regression analyses were applied to WMH volume changes in separate white matter regions, both periventricular and deep WMH volume changes were significantly associated with MRIR (periventricular region, $P < .001$; deep region, $P = .004$), MMPI (periventricular region, $P = .035$; deep region, $P = .044$), and baseline WMH volumes ($P < .001$ for both regions) of each relevant region. However, MRIR showed a stronger association with WMH progression

Table 2

Correlation Coefficiencies of Continuous Variables with WMH Progression

Variable	WMH Volume Change	P Value
Age	0.278	<.001*
Baseline WMH volume	0.433	<.001*
MR imaging interval (mo)	0.003	.954
MRIR	0.328	<.001*
MMPI	0.275	<.001*

* $P < .01$.

Table 3

Univariate Analyses for Categorical Parameters Associated with WMH Progression

Variable	WMH Volume Change (mL)		P Value
	Yes	No	
Clinical parameter			
Male sex	4.66 ± 7.73	3.77 ± 7.00	.398
Previous lacunar infarction	6.17 ± 9.05	3.33 ± 6.53	.002*
Hypertension	4.96 ± 8.16	2.48 ± 5.36	<.001*
Diabetes mellitus	5.67 ± 9.53	3.34 ± 6.02	.008*
Coronary heart disease	5.20 ± 1.10	3.92 ± 6.80	.251
Smoking in past 5 years	4.79 ± 6.02	3.98 ± 7.51	.469
Hyperlipidemia	5.19 ± 9.67	3.48 ± 5.75	.045†
Use of statins	4.32 ± 7.94	3.76 ± 6.64	.423
ACEi or ARB use	5.15 ± 8.51	3.18 ± 6.15	.006*
Use of antiplatelet agents	4.49 ± 7.75	2.76 ± 5.84	.014†
Indication for work-up			
Medical check-up	3.59 ± 7.01	4.40 ± 7.59	.250
Headache or dizziness	3.02 ± 5.95	4.43 ± 7.78	.075
Small unruptured intracranial aneurysm‡	6.17 ± 9.05	3.33 ± 6.53	.002*
Old lacunar infarction	3.09 ± 5.82	4.14 ± 7.47	.411

Note.—Unless otherwise indicated, data are mean \pm standard deviation.

* $P < .01$.

† $P < .05$.

‡ Patients with a recent diagnosis of intracranial aneurysm at baseline MR imaging or MR angiography were included.

in periventricular regions than in deep white matter regions (Table 4). In every linear regression analysis, variance inflation factor values for each variable were less than 1.500. When the study population was divided into subgroups according to MRIR values of less than 0.940, 0.940–0.969, 0.970–0.999, and 1.000 or more, the higher MRIR values appeared to be associated with increased progression of both periventricular and deep WMH volumes. Notably, MRIR greater than 1.000 was associated with markedly increased WMH progression (mean, $6.07 \text{ mL} \pm 6.61$ vs $1.77 \text{ mL} \pm$

4.63 in the periventricular region and $1.57 \text{ mL} \pm 1.77$ vs $0.60 \text{ mL} \pm 1.52$ in the deep white matter region; $P < .001$ for both) (Fig 3). In addition, the physiologic base that shows MRIR can reflect the compliance of the cerebral penetrating arterioles is shown in Figure 4.

Discussion

In this study, we used a noninvasive method in a fairly large population to show that a sonographic index MRIR might reflect the pulsation of penetrating arteries and that it is independently

Table 4
Linear Regression Analyses for WMH Volume Change

Variable	Unstandardized Coefficient	Standardized Coefficient	PValue	Variance Inflation Factor
Total WMH volume change*	-37.122 (-50.863, 23.381)	...	<.001 [†]	...
Age [‡]	0.075 (-0.009, 0.159)	0.084	.078	1.349
Baseline WMH volume [‡]	1.275 (0.868, 1.682)	0.293	<.001 [†]	1.349
MRIR [‡]	30.608 (16.641, 44.574)	0.189	<.001 [†]	1.143
MMPI [‡]	4.342 (0.259, 8.426)	0.099	.037 [§]	1.344
Lacunar stroke history	0.774 (-0.674, 2.221)	0.046	.294	1.148
Hypertension	0.555 (-0.947, 2.057)	0.036	.468	1.484
Diabetes mellitus	0.823 (-0.541, 2.187)	0.052	.236	1.135
Hyperlipidemia	0.665 (-0.622, 1.951)	0.043	.311	1.061
Use of ACEi or ARB	0.045 (-1.403, 1.494)	0.003	.951	1.477
Use of antiplatelet agents	-0.414 (-1.894, 1.067)	-0.024	.583	1.153
Periventricular WMH volume change	-30.886 (-41.498, 20.274)	...	<.001 [†]	...
Age [‡]	0.060 (-0.004, 0.125)	0.087	.067	1.347
Baseline WMH volume ^{‡#}	0.980 (0.657, 1.303)	0.282	<.001 [†]	1.339
MRIR [‡]	26.021 (15.252, 36.790)	0.207	<.001 [†]	1.140
MMPI [‡]	3.384 (0.232, 6.536)	0.100	.035 [§]	1.344
Lacunar stroke history	0.630 (-0.488, 1.747)	0.048	.269	1.147
Hypertension	0.459 (-0.701, 1.619)	0.039	.437	1.484
Diabetes mellitus	0.618 (-0.435, 1.670)	0.050	.250	1.135
Hyperlipidemia	0.492 (-0.502, 1.485)	0.041	.331	1.061
ACEi or ARB use	0.049 (-1.069, 1.167)	0.004	.931	1.478
Use of antiplatelet agents	-0.281 (-1.424, 0.862)	-0.021	.630	1.153
Deep WMH volume change ^{**}	-5.841 (-9.073, 2.608)	...	<.001 [†]	...
Age [‡]	0.016 (-0.003, 0.036)	0.080	.100	1.348
Baseline WMH volume ^{‡††}	0.274 (0.189, 0.358)	0.310	<.001 [†]	1.360
MRIR [‡]	4.775 (1.536, 8.013)	0.129	.004 [†]	1.148
MMPI [‡]	0.970 (0.026, 1.915)	0.098	.044 [§]	1.344
Lacunar stroke history	0.162 (-0.173, 0.497)	0.042	.344	1.149
Hypertension	0.104 (-0.244, 0.451)	0.030	.558	1.484
Diabetes mellitus	0.203 (-0.112, 0.519)	0.056	.206	1.135
Hyperlipidemia	0.179 (-0.119, 0.477)	0.051	.239	1.061
ACEi or ARB use	0.001 (-0.334, 0.336)	0.000	.997	1.477
Use of antiplatelet agents	-0.124 (-0.467, 0.218)	-0.032	.477	1.152

Note.—Data in parentheses are 95% confidence intervals.

* $R^2 = 0.262, P < .001$.

[†] $P < .01$.

[‡] The variables were log transformed to obtain a normal distribution.

[§] $P < .05$.

^{||} $R^2 = 0.267, P < .001$.

[#] Baseline periventricular WMH volume.

^{**} $R^2 = 0.237, P < .001$.

^{††} Baseline deep WMH volume.

associated with WMH progression. Remarkably, the relationship of MRIR with WMH progression was stronger than that of any previously established risk factor for WMH progression, including increased age and hypertension (1–4). These data suggest that decreased

pulsatility in perforating arteries plays a fundamental role in WMH progression and that age, hypertension, and medication effects may be indirectly related to WMH progression via arterial compliance (7,8,12). Furthermore, association of MRIR and WMH progression

was valid in both the periventricular region and the deep white matter, although the association was higher for periventricular WMH progression. This may be explained by the fact that most of the periventricular region is directly supplied by M1 perforating arteries,

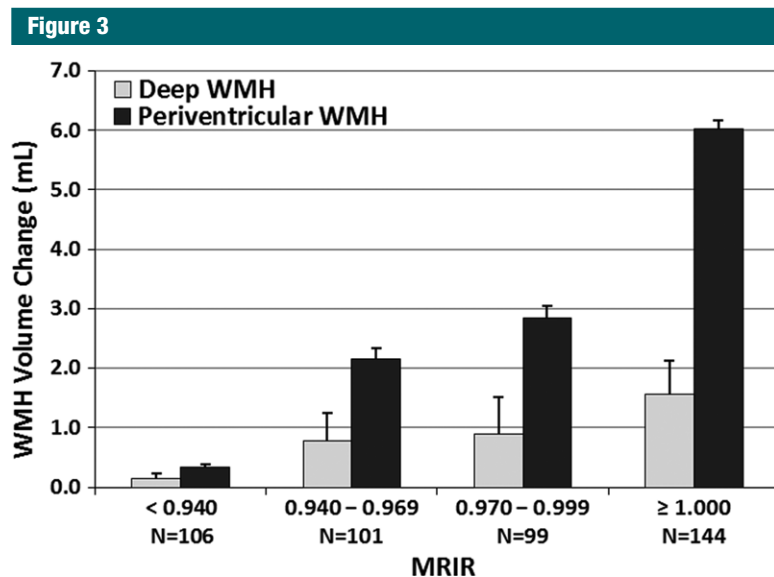


Figure 3: Profiles of WMH volume change according to MRIR values. Horizontal lines above the bars denote standard errors.

whereas the deep white matter region is partly supplied by cortical penetrating arteries (19). Additionally, we observed that baseline WMH volume and PI of M1 were also independently related to WMH progression, which is consistent with the findings of previous studies (2,5,15).

Numerous studies have investigated markers for the severity or progression of WMH, including the parameters for systemic arterial stiffness, such as pulse pressure and aortic pulse wave velocities (13,14). However, relative to these markers, MRIR has the advantage of directly reflecting cerebral penetrating arterial compliance. Accordingly, MRIR has a closer relationship to the underlying pathologic mechanisms that may enable it to be used in clinical practice to predict or monitor long-term WMH progression. Furthermore, an MRIR cutoff value could be used as an indicator of diminished cerebral microvascular compliance, as MRIR of 1.000 or greater was highly associated with more significant WMH progression in this study.

The reflection of penetrating arterial compliance by MRIR is based on the distinct physiologic properties of the penetrating arteries compared with those of the pial vessels. The penetrating arteries are much more

pulsatile than the pial arteries, and they consume most of the pulse pressure of the arterial system (8,31). In particular, for the perforating arteries that ramify directly from the M1 stem, increased intravascular pressure in M1 derived with a systolic pulse is directly delivered to them. As the perforating arteries are highly compliant (8,9,31), increased intraluminal pressure actively dilates those arteries, inducing marked reduction of resistance (32,33) and ultimately augmenting flow distribution in the perforating artery territories during systolic phases. In contrast, pial vessels such as M1 have large diameters and low resistance, and their diameter changes only minimally with changes in intraluminal pressure during a pulse cycle (16). Thus, resistance change in M1 during a pulse cycle is negligible, and the amount of flow variation approximates the flow velocity changes. An in vitro study of the murine MCA and its penetrating arterioles showed that incremental changes in intravascular pressure significantly increase the diameter of the penetrating arterioles, whereas the pial arteries do not dilate (34). Additionally, a study using phase-contrast MR imaging reported significant dampening of PI along the M1; this dampening is not observed in

the internal carotid artery (17), further supporting the variation in perforating territory-specific pulsatile flow.

This enables MRIR to reflect dynamic alterations of flow distribution in perforating arteries. If F is flow in proximal M1, f is flow in M1 perforators at diastole, and ΔF and Δf are additional flow volumes delivered by a systolic pulse, RI of proximal M1 (RI_p) and distal M1 (RI_d) would be approximately as follows:

$$RI_p \approx \frac{\Delta F}{F + \Delta F}, RI_d \approx \frac{\Delta F - \Delta f}{(F - f) + \Delta F - \Delta f}$$

$$= \frac{\Delta F(1 - r \times \frac{f}{F})}{F(1 - \frac{f}{F}) + \Delta F(1 - r \times \frac{f}{F})}, r = \frac{\Delta f}{f} \cdot \frac{\Delta F}{F}$$

When the perforating arteries are compliant, r would be greater than 1 per the increased proportion of flow in the perforating artery territory, and MRIR would be less than 1. As r increases along the increasing arterial compliance, MRIR would be lower. In this case, the compliant lumen markedly dilates to attenuate the velocity and shear rate increment in the penetrating arterioles (31), inducing effective transformation of a systolic pulse into an elastic vessel pulsation that ultimately facilitates solute clearance via the glymphatic system (7,8,10,12). However, when the perforating arteries are stiff, the increase in velocity should be maximized to compensate for impaired lumen dilatation. Additionally, the effective blood viscosity, which has a strong inverse correlation with arteriolar luminal diameters, would maintain a high value (33). Consequently, shear rate would be markedly increased, inducing early wastage of the pulse energy (32). The flow capacity of the M1 perforators might be restricted and would be reduced, even to less than 1, resulting in a higher MRIR. These arteries would accordingly lack the capacity for solute clearance (7,8,12). Additionally, highly fluctuating shear stress might exacerbate endothelial dysfunction (1,17,35), vascular inflammation (1,35), and blood brain barrier disruption (17), and it ultimately might enhance WMH progression.

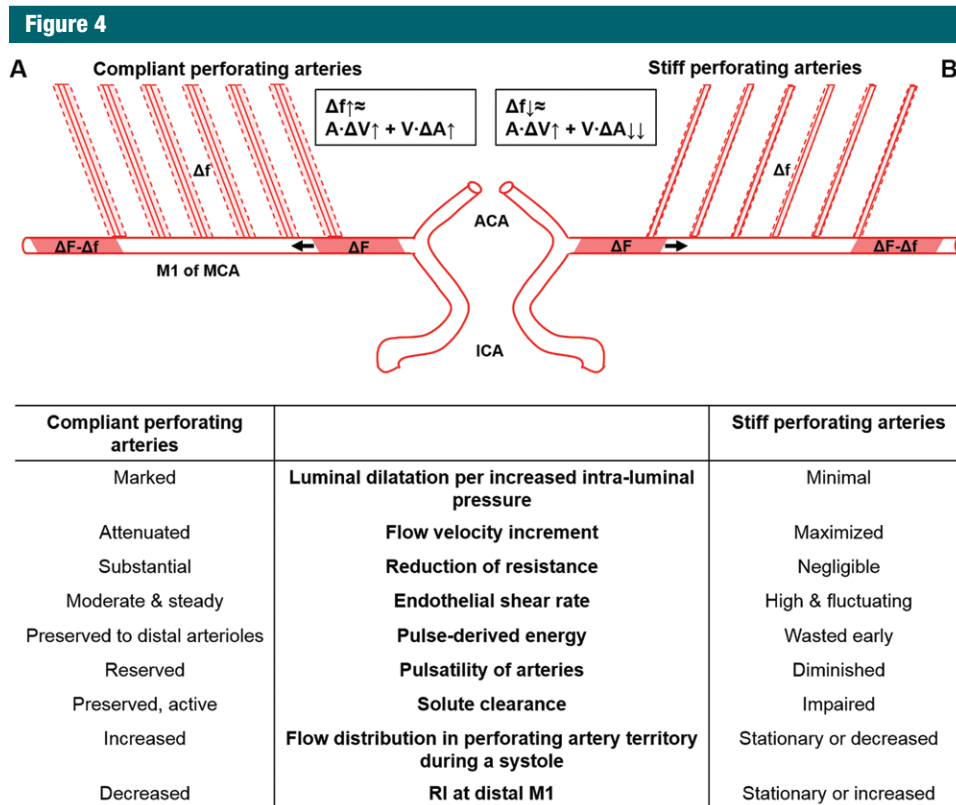


Figure 4: Schematic of physiologic base of MRIR. *A* and *B* show physiologic consequences derived by compliant or stiff M1 perforating arteries, respectively. Formulas in rectangles describe relative amount of variations in flow volume, lumen area, and flow velocity in a perforating artery, derived by a systolic pulse. Dashed parallelograms denote the dilation capacity of arteries according to intraluminal pressure increments. *F* denotes flow in proximal M1; *f*, M1 perforators at diastole; *A*, the lumen area; and *V*, flow velocity of the perforating arteries. Δ = additional value of each variable delivered by a systolic pulse, *ACA* = anterior cerebral artery, *ICA* = internal carotid artery.

Several limitations of our study should be addressed. First, the accuracy of measurement, operator dependency, and the normal range of the MRIR is not fully established. Second, the reproducibility of MRIR, which might be essential to validate its clinical utility, was evaluated with only 20 pairs of TCD evaluations. Third, due to a retrospective study design, patients with heterogeneous clinical profiles and indications for MR imaging and TCD evaluations were included in the study population. This might raise an issue of selection bias. However, the potential sources of bias were limited by implementation of the exclusion criteria. Furthermore, none of the indications of initial MR imaging or TCD evaluation showed a significant association with WMH progression volume.

To establish the clinical utility of MRIR, future prospective studies should endeavor to validate and expand our findings by applying a standardized follow-up protocol and including data reproducibility evaluations. Furthermore, comparative analyses of MRIR with more direct measurements of cerebral microvascular pulsatility (31) or other markers of arterial compliance might elucidate the pathophysiologic relationship of microvascular compliance and WMH progression.

Disclosures of Conflicts of Interest: W.J.L. disclosed no relevant relationships. K.H.J. disclosed no relevant relationships. Y.J.R. disclosed no relevant relationships. K.J.L. disclosed no relevant relationships. J.M.K. disclosed no relevant relationships. S.T.L. disclosed no relevant relationships. K.C. disclosed no relevant relationships. M.K. disclosed no relevant relationships. S.K.L. disclosed no relevant relationships. J.K.R. disclosed no relevant relationships.

References

1. Pantoni L. Cerebral small vessel disease: from pathogenesis and clinical characteristics to therapeutic challenges. *Lancet Neurol* 2010;9(7):689–701.
2. Godin O, Tzourio C, Maillard P, Mazoyer B, Dufouil C. Antihypertensive treatment and change in blood pressure are associated with the progression of white matter lesion volumes: the Three-City (3C)-Dijon Magnetic Resonance Imaging Study. *Circulation* 2011;123(3):266–273.
3. Breteler MM, van Swieten JC, Bots ML, et al. Cerebral white matter lesions, vascular risk factors, and cognitive function in a population-based study: the Rotterdam study. *Neurology* 1994;44(7):1246–1252.
4. Longstreth WT Jr, Arnold AM, Beauchamp NJ Jr, et al. Incidence, manifestations, and predictors of worsening white matter on serial cranial magnetic resonance imaging in the elderly: the Cardiovascular Health Study. *Stroke* 2005;36(1):56–61.

5. Gouw AA, van der Flier WM, Fazekas F, et al. Progression of white matter hyperintensities and incidence of new lacunes over a 3-year period: the Leukoaraiosis and Disability study. *Stroke* 2008;39(5):1414–1420.
6. Sachdev P, Wen W, Chen X, Brodaty H. Progression of white matter hyperintensities in elderly individuals over 3 years. *Neurology* 2007;68(3):214–222.
7. Joutel A, Monet-Leprêtre M, Gosele C, et al. Cerebrovascular dysfunction and microcirculation rarefaction precede white matter lesions in a mouse genetic model of cerebral ischemic small vessel disease. *J Clin Invest* 2010;120(2):433–445.
8. Kress BT, Iliff JJ, Xia M, et al. Impairment of paravascular clearance pathways in the aging brain. *Ann Neurol* 2014;76(6):845–861.
9. Wardlaw JM, Smith C, Dichgans M. Mechanisms of sporadic cerebral small vessel disease: insights from neuroimaging. *Lancet Neurol* 2013;12(5):483–497.
10. Weller RO, Hawkes CA, Kalra RN, Werring DJ, Carare RO. White matter changes in dementia: role of impaired drainage of interstitial fluid. *Brain Pathol* 2015;25(1):63–78.
11. Bude RO, Rubin JM. Relationship between the resistive index and vascular compliance and resistance. *Radiology* 1999;211(2):411–417.
12. Iliff JJ, Wang M, Zeppenfeld DM, et al. Cerebral arterial pulsation drives paravascular CSF-interstitial fluid exchange in the murine brain. *J Neurosci* 2013;33(46):18190–18199.
13. Mitchell GF, van Buchem MA, Sigurdsson S, et al. Arterial stiffness, pressure and flow pulsatility and brain structure and function: the Age, Gene/Environment Susceptibility–Reykjavik study. *Brain* 2011;134(Pt 11):3398–3407.
14. Scuteri A, Wang H. Pulse wave velocity as a marker of cognitive impairment in the elderly. *J Alzheimers Dis* 2014;42(Suppl 4):S401–S410.
15. Webb AJ, Simoni M, Mazzucco S, Kuker W, Schulz U, Rothwell PM. Increased cerebral arterial pulsatility in patients with leukoaraiosis: arterial stiffness enhances transmission of aortic pulsatility. *Stroke* 2012;43(10):2631–2636.
16. Giller CA, Bowman G, Dyer H, Mootz L, Krippner W. Cerebral arterial diameters during changes in blood pressure and carbon dioxide during craniotomy. *Neurosurgery* 1993;32(5):737–741; discussion 741–742.
17. Zarrinkoob L, Ambarki K, Wählin A, et al. Aging alters the dampening of pulsatile blood flow in cerebral arteries. *J Cereb Blood Flow Metab* 2016;36(9):1519–1527.
18. Lindegaard KF, Lundar T, Wiberg J, Sjøberg D, Aaslid R, Nornes H. Variations in middle cerebral artery blood flow investigated with noninvasive transcranial blood velocity measurements. *Stroke* 1987;18(6):1025–1030.
19. Marinkovic SV, Milisavljevic MM, Kovacevic MS, Stevic ZD. Perforating branches of the middle cerebral artery: microanatomy and clinical significance of their intracerebral segments. *Stroke* 1985;16(6):1022–1029.
20. Ovbiagele B, Saver JL. Cerebral white matter hyperintensities on MRI: current concepts and therapeutic implications. *Cerebrovasc Dis* 2006;22(2-3):83–90.
21. Aaslid R, Markwalder TM, Nornes H. Non-invasive transcranial Doppler ultrasound recording of flow velocity in basal cerebral arteries. *J Neurosurg* 1982;57(6):769–774.
22. Nicoletto HA, Burkman MH. Transcranial Doppler series part II: performing a transcranial Doppler. *Am J Electroneurodiagn Technol* 2009;49(1):14–27.
23. Bash S, Villablanca JP, Jahan R, et al. Intracranial vascular stenosis and occlusive disease: evaluation with CT angiography, MR angiography, and digital subtraction angiography. *AJNR Am J Neuroradiol* 2005;26(5):1012–1021.
24. Nederkoorn PJ, Elgersma OE, van der Graaf Y, Eikelboom BC, Kappelle LJ, Mali WP. Carotid artery stenosis: accuracy of contrast-enhanced MR angiography for diagnosis. *Radiology* 2003;228(3):677–682.
25. Samuels OB, Joseph GJ, Lynn MJ, Smith HA, Chimowitz MI. A standardized method for measuring intracranial arterial stenosis. *AJNR Am J Neuroradiol* 2000;21(4):643–646.
26. Sadikin C, Teng MM, Chen TY, et al. The current role of 1.5T non-contrast 3D time-of-flight magnetic resonance angiography to detect intracranial steno-occlusive disease. *J Formos Med Assoc* 2007;106(9):691–699.
27. Inzitari D, Pracucci G, Poggesi A, et al. Changes in white matter as determinant of global functional decline in older independent outpatients: three year follow-up of LADIS (leukoaraiosis and disability) study cohort. *BMJ* 2009;339:b2477.
28. ten Dam VH, van den Heuvel DM, de Craen AJ, et al. Decline in total cerebral blood flow is linked with increase in periventricular but not deep white matter hyperintensities. *Radiology* 2007;243(1):198–203.
29. van den Heuvel DM, ten Dam VH, de Craen AJ, et al. Increase in periventricular white matter hyperintensities parallels decline in mental processing speed in a non-demented elderly population. *J Neurol Neurosurg Psychiatry* 2006;77(2):149–153.
30. Meng D, Hosseini AA, Simpson RJ, et al. Lesion topography and microscopic white matter tract damage contribute to cognitive impairment in symptomatic carotid artery disease. *Radiology* 2017;282(2):502–515.
31. Bouvy WH, Geurts LJ, Kuijf HJ, et al. Assessment of blood flow velocity and pulsatility in cerebral perforating arteries with 7-T quantitative flow MRI. *NMR Biomed* 2016;29(9):1295–1304.
32. Pyke KE, Tschakovsky ME. The relationship between shear stress and flow-mediated dilatation: implications for the assessment of endothelial function. *J Physiol* 2005;568(2):357–369.
33. Pries A, Secomb TW, Gessner T, Sperandio M, Gross J, Gaetgens P. Resistance to blood flow in microvessels in vivo. *Circ Res* 1994;75(5):904–915.
34. Cipolla MJ, Li R, Vitullo L. Perivascular innervation of penetrating brain parenchymal arterioles. *J Cardiovasc Pharmacol* 2004;44(1):1–8.
35. Tzima E, Irani-Tehrani M, Kiosses WB, et al. A mechanosensory complex that mediates the endothelial cell response to fluid shear stress. *Nature* 2005;437(7057):426–431.